Development, Verification and KPI Analysis of Infrastructure-Assisted Trajectory Planners

Martin Rudigier
Control Systems Group
Virtual Vehicle Research GmbH
Graz, Austria
martin.rudigier@v2c2.at

Selim Solmaz*
Control Systems Group
Virtual Vehicle Research GmbH
Graz, Austria
selim.solmaz@v2c2.at

Georg Nestlinger
Control Systems Group
Virtual Vehicle Research GmbH
Graz, Austria
georg.nestlinger@v2c2.at

Kailin Tong
Control Systems Group
Virtual Vehicle Research GmbH
Graz, Austria
kailin.tong@v2c2.at

2022 International Conference on Connected Vehicle and Expo (ICCVE) | 978-1-6654-1687-0/22/$31.00 ©2022 IEEE | DOI: 10.1109/ICCVE52871.2022.9742783

***Abstract*—Automated vehicles are expected to cause a paradigm shift in mobility and the way we travel. Particularly, the increasing penetration rates of vehicles with automated driving functions will introduce new challenges such as excessive rutting. Lack of wheel wander and keeping to the lane center perfectly is expected to lead to excessive road surface depression induced by automated vehicle platoons. Inspired by this, the EU project ESRIUM investigates infrastructure assisted routing recommendations. In this respect, specially designed ADAS functions are being developed with capabilities to adapt their behavior according to specific routing recommendations, which will help to reduce rutting as well as to improve safety. The current paper presents three rule-based trajectory planner design alternatives for a representative use case and, their performance comparisons based on a simulation framework.**

***Index Terms*—automated vehicles; ADAS/AD functions; C-ITS; IVIM; infrastructure assistance; routing recommendations**

I. Introduction

Automated driving and ADAS (advanced driver assistance systems) are becoming more widespread with the promise of increased safety and convenience. These are direct consequences of the reduction the cognitive load of the driver. There are however many hurdles to be cleared before realizing highly automated or fully autonomous driving. The main challenge here is to guarantee safety in every possible traffic condition. This is particularly important for the transition phase from conventional to autonomous traffic, where automated vehicles with varying autonomy levels need to coexist with conventional vehicles [1], [2].

The widely accepted SAE J3016 norm [3] defines the levels of autonomy for autonomous vehicles. According to this taxonomy, the most advanced automated vehicles we have on the road today are classified as SAE Level-3 or lower, which implies that the driver holds the main responsibility and liability. All the decision-making processes of such vehicles depend on the computations performed on the ego vehicle, utilizing only on-board sensors, similar to the perception process of a human driver. However, for higher levels of autonomy (SAE Level-4 and Level-5), infrastructure assistance will be necessary to ensure partial or full liability of the driving safety. In the simplest terms, infrastructure communication can be utilized to convey the dynamic traffic and hazard information ahead and beyond the range of on-board sensors in the form of real-time routing and driving recommendations for CAVs (connected automated vehicles). CAVs and especially heavy-duty trucks in automated platoon formations, are per design expected to have no wheel wander. These will lead to more road damage in the form of rutting of the road surface, and consequently to infrastructure maintenance issues, as the penetration of such vehicles increase.

Motivated by this, the EU-H2020 project ESRIUM [4] aims for the high-level objective of increased safety and resource efficiency of road transport on European roads. In doing this, its key innovation is a digital map of road surface damage and road wear. This shall help reduce both the number of road works and the associated problems by using new digital services for managing the traffic, as well as by controlling the utilization of the road. The road wear map will contain unique information for the road operators to enhance the road maintenance planning, as well as to provide routing and driving recommendations for connected vehicles utilizing C-ITS communications. These recommendations can be used for adjusting the driving path (within and between lanes), which shall help with the graceful wear of the road surface, thereby reducing the regular maintenance actions. Particularly, optimization strategies using infrastructure recommendations are proposed as illustrated in two specific scenarios in Figure 1, particularly for a desired in-lane offset as well as to initiate informed lane changes to avoid potential hazard situations. For this purpose, specially designed ADAS functions (i.e., lateral and longitudinal tracking controllers and trajectory planners)

This work was conducted in the scope of the ESRIUM Project, which has received funding from the EUSPA as part of EU-Horizon 2020 research and innovation programme under grant agreement No 101004181.

*Corresponding author. Tel: +43 316 873 9730, Fax: +43 316 873 9602.

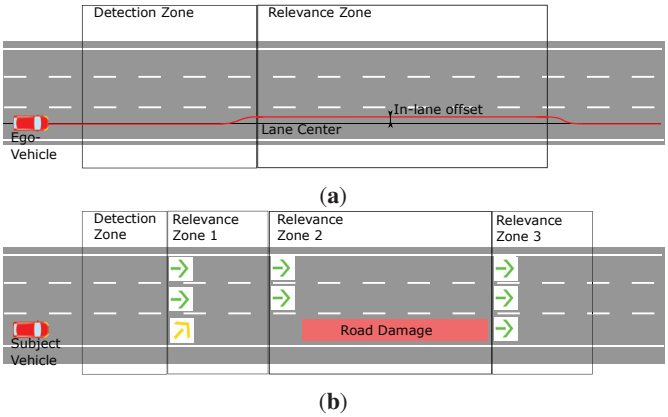

Fig. 1: Use-case scenario specification for (**a**) in-lane offset recommendation and (**b**) lane change recommendations [5].

are developed with capabilities to adapt their behavior according to specific routing and driving recommendations received in the form of infrastructure to vehicle information message (IVIM).

As a follow-up paper to [5], the current paper presents the comparison of three alternative transition curves for a rule-based trajectory planner. A set of performance indicators serves as a basis for their selection for the described infrastructure-assisted routing recommendations for the corresponding scenarios. Also, the specific use case scenario to be tested on the public road was implemented utilizing the UHDmaps® [6] of the road network in a simulation framework. Consequently, the evaluation results are presented.

We note here that the introduced rule-based trajectory planner with different transition curves is rather a simple solution for motorway driving conditions, where the variability in the driving conditions are limited. The utilization of such a trajectory planner is simply motivated by the use case of the ESRIUM project, where an infrastructure signal is used to trigger a certain behavior of the driving function. For this purpose a self-developed rule-based planner was therefore developed, which is real-time capable and is simpler to implement together with infrastructure recommendations.

II. Simulation Setup

A co-simulation environment based on Matlab/Simulink and the vehicle dynamics software IPG-CarMaker 10 was utilized for developing the driving functions as shown in Fig. 2. This simulation environment was preferred since it is well suited for rapid-prototyping purposes. The driving functions here consist of the trajectory planner, as well as longitudinal and lateral tracking controllers that are implemented in Matlab/Simulink. The trajectory planner requires an object list information including the lane markings. The controllers require the vehicle state and a longitudinal or lateral reference trajectory respectively. The vehicle state includes actuation signals (steering angle, brake and gas pedal), as well as velocities and accelerations. For the object list, no sensor dynamics were assumed considering only occlusion effects. Lane markings are represented using third order polynomials and related polynomial domains.

The routing recommendations based on IVIM messages were implemented as preset messages as indicated in Fig. 2. Future real-life demonstrations will be performed on the Austrian A2 motorway section near Graz as indicated in Fig. 3. Therefore, the corresponding UHDmap® [6] in the OpenDRIVE format was used in the CarMaker driving scenario setup.

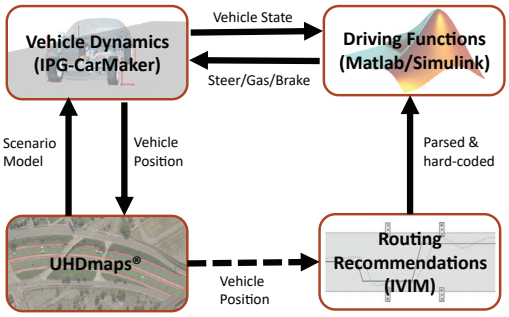

Fig. 2: Co-simulation architecture utilizing Matlab/Simulink and IPG Carmaker 10.

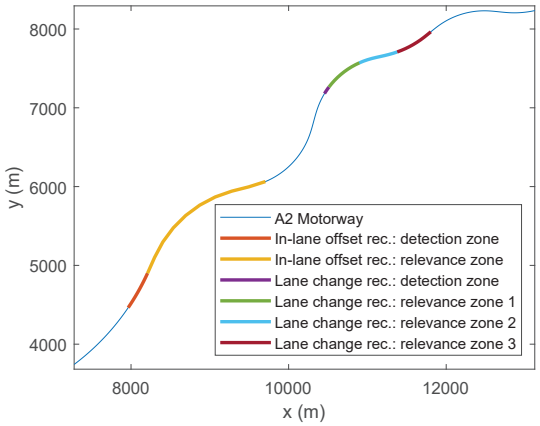

Fig. 3: UHDmap® of the Austrian A2 Motorway section near Graz with overlay of detection and relevance zones and corresponding recommendations as used in the test scenario.

Fig. 3 shows the stretch of the A2 where this simulation tests were conducted. The simulated vehicle starts in the southeastern corner and drives to northwestern corner. During this test scenario the automated vehicle receives two different IVIMs. The first IVIM contains an in-lane offset recommendation of $40\,\mathrm{cm}$ to the left (Fig. 1a), and the second a lane change recommendation (Fig. 1b). The ego vehicle drives with $130\,\mathrm{km/h}$ and and the shown results are without surrounding traffic.

III. Comparison of Polynomial- and Bezier-Type Transition Curves for the Trajectory Planning

Trajectory planning is an essential part to realize high level automated driving [7]. A simple but important solution for the

trajectory planning problem involves the use of an interpolating curve planner. Such a planner is normally integrated into a hierarchical planning system and combined with a rule-based behavior planner [8]. One well-known work in this direction is the optimal trajectory generator using quintic polynomials in a Frenet frame, which can be incorporated into the decision-making layer [9]. Furthermore, OpenPlanner of Autoware extends this planning scheme for on-road verification. A global planner firstly provides an initial route. Next, the local planning module produces a set of local roll-outs varied from a reference path, and a behavior generator function taking account of driving semantics, finally selects an optimal local trajectory and generates a velocity profile [10].

The solution used in this paper for the trajectory planning problem was introduced in a recent paper by the authors [5]. The developed trajectory planner (TP) is designed for driving on highway with well defined lane-markings and it steers the vehicle to the middle of the rightmost lane unless an external lane-change or in-lane offset recommendation is received. If a lane change is triggered, a set of rules is checked to ensure that there is a valid lane to change to, and the lane change is safe to conduct. In doing so it checks that it does not hinder the surrounding traffic e.g. by forcing an upcoming vehicle to brake suddenly. A lane change can be triggered by a slower vehicle driving in front of the ego vehicle or if the ego vehicle is not driving on the rightmost lane, while the rightmost lane is free, or by an external input (e.g. IVIM with lane change recommendation).

The algorithm utilized in this case was a rule based trajectory planner adapted to utilize C-ITS messages such as the in-lane offset recommendation and the lane change recommendation (see Fig. 1 as well as the detailed description of the use cases in [5]). There, the lane change curves were constructed utilizing two quadratic Bezier curves connected by a straight line. Here we consider two other transition curves as an alternative, namely a 5th order polynomial as well as a link of two 4th order polynomials connected by a straight line. We describe these next.

A. Bezier Curve Construct

Fig. 4 shows the construction of the local lane change trajectory in Frenet coordinates. The Bezier curve from P_1 to P_2 (red) is connected via the straight line from P_2 to Q_1 (magenta) to the second Bezier curve from Q_1 to Q_2 (blue). This specific approach is also described in detail in [5]. It is motivated due to the lack of the ability to provide trustworthy lane information from the lane detection sensor on the actual test vehicle (which is a Mobileye intelligent camera). Particularly the lane width information for the neighboring lanes are not known with sufficient accuracy. To overcome this issue, the planned path consists of two quadratic Bézier curves connected via a straight segment that can be lengthened or shortened if the actual lane width of the target lane differs from the estimated lane width.

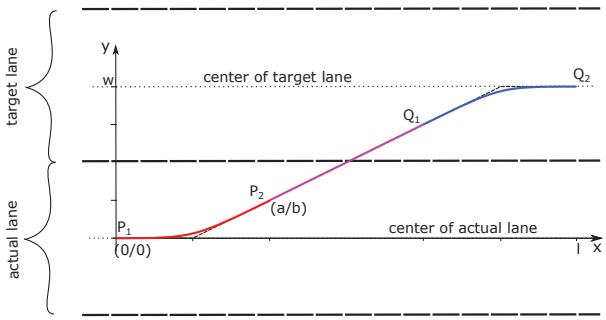

Fig. 4: Lane change path construction utilizing two quadratic Bezier curves [5].

B. Fifth Order Polynomial

As an alternative solution, a 5^{th} order polynomial

$$y(x) = p_0 + p_1 x + p_2 x^2 + p_3 x^3 + p_4 x^4 + p_5 x^5 \tag{1}$$

was chosen. Again the local trajectory was planned in Frenet coordinates. To get a smooth path, the first and second derivatives were set to zero

$$y_0' = 0, \quad y_0'' = 0, \quad y_1' = 0, \quad y_1'' = 0 \tag{2}$$

at the terminal points $y(x_0) = 0$ and $y(x_1) = w$ of the curve. In accordance with Fig. 4, $x_0 = 0$ and $x_1 = l$.

In total we get six equations for the six unknown polynomial coefficients. These equations can be arranged in matrix form

$$\begin{aligned} \mathbf{p} &= \begin{bmatrix} p_5 & p_4 & p_3 & p_2 & p_1 & p_0 \end{bmatrix}^\mathsf{T} \\ \mathbf{y} &= \begin{bmatrix} 0 & w & 0 & 0 & 0 & 0 \end{bmatrix}^\mathsf{T} \\ \mathbf{A_1} &= \begin{bmatrix} x_0^5 & x_0^4 & x_0^3 & x_0^2 & x_0 & 1 \\ x_1^5 & x_1^4 & x_1^3 & x_1^2 & x_1 & 1 \\ 5x_0^4 & 4x_0^3 & 3x_0^2 & 2x_0 & 1 & 0 \\ 5x_1^4 & 4x_1^3 & 3x_1^2 & 2x_1 & 1 & 0 \\ 20x_0^3 & 12x_0^2 & 6x_0 & 2 & 0 & 0 \\ 20x_1^3 & 12x_1^2 & 6x_1 & 2 & 0 & 0 \end{bmatrix} \end{aligned} \tag{3}$$

and solved via matrix inversion

$$\mathbf{p} = \mathbf{A}_1^{-1}\mathbf{y}. \tag{4}$$

Equation (4) must be solved each time a new lane change curve is triggered. This solution lacks the possibility to react to a corrupted lane width information without recalculating (4), but results in a smoother steering wheel angle curve.

C. Fourth Order Polynomial Construct

The third transition curve is constructed by replacing the Bezier curves in Figure 4 with 4th order polynomials

$$y(x) = p_0 + p_1 x + p_2 x^2 + p_3 x^3 + p_4 x^4. \tag{5}$$

At point P_1, the first and second derivatives are set to zero, which is achieved with the boundary conditions below:

$$x_0 = 0, \quad y_0 = 0, \quad y_0' = 0, \quad y_0'' = 0. \tag{6}$$

As seen in Fig. 4, the first derivative should be the slope of the connecting straight at $P_1 = (a, b)$. The second derivative is again set to zero as below:

$$x_1 = a, \quad y_1 = b, \quad y_1' = \frac{w - 2b}{l - 2a}, \quad y_1'' = 0. \tag{7}$$

With the end point (a, b) of the polynomial and five polynomial coefficients there are seven unknown parameters in total but only six equations. Therefore, a is set to $1.5\,\mathrm{s}$ which equals a third of the chosen standard lane change duration of $4.5\,\mathrm{s}$. Equation (8) below combines equations (5) to (7) in a matrix form and constitutes the 4^{th} order construct that has to be solved each time a lane change path is computed utilizing

$$\begin{aligned}
\mathbf{q} &= \begin{bmatrix} p_4 & p_3 & p_2 & p_1 & p_0 & b \end{bmatrix}^\mathsf{T} \\
\mathbf{z} &= \begin{bmatrix} 0 & 0 & 0 & \frac{w}{l-2a} & 0 & 0 \end{bmatrix}^\mathsf{T} \\
\mathbf{A_2} &= \begin{bmatrix}
x_0^4 & x_0^3 & x_0^2 & x_0 & 1 & 0 \\
x_1^4 & x_1^3 & x_1^2 & x_1 & 1 & -1 \\
4x_0^3 & 3x_0^2 & 2x_0 & 1 & 0 & 0 \\
4x_1^3 & 3x_1^2 & 2x_1 & 1 & 0 & \frac{2}{l-2a} \\
12x_0^2 & 6x_0 & 2 & 0 & 0 & 0 \\
12x_1^2 & 6x_1 & 2 & 0 & 0 & 0
\end{bmatrix}
\end{aligned} \tag{8}$$

which are then solved using the matrix equation

$$\mathbf{q} = \mathbf{A_2}^{-1}\mathbf{z} \tag{9}$$

IV. KPI DEFINITIONS BASED ON THE FUNCTIONAL REQUIREMENTS

Here we define the basic performance indicators that were used to compare the three types of transition curves from the previous section. These KPIs are selected taking into account the specific use case scenarios shown in Figure 1. The specific KPIs are given in Table I, which stem from the functional requirements of the driving functions.

TABLE I: Key performance indicators for the comparison of the rule-based trajectory planners.

KPI Designation	**Performance Specification**		
	Definition	***Performance***	***Unit***
KPI-1	Maximum longitudinal velocity tracking error from set-point	5	$\mathrm{km/h}$
KPI-2	Maximum lateral position overshoot from set-point	20	cm
KPI-3	Minimum safety distance from road lane border	20	cm
KPI-4	Maximum allowed longitudinal acceleration/ decleration*	2/3.5	$\mathrm{m/s^2}$
KPI-5	Maximum allowed lateral acceleration**	4	$\mathrm{m/s^2}$

* according to ISO 15622:2018 standard (for $130\,\mathrm{km/h}$).
** according to ISO 21202:2020 standard (for light-duty vehicles).

In literature, a wide variety of lateral path tracking error definitions is used. According to [11], those can be categorized by vehicle reference (e.g. center of gravity), look-ahead direction and distance and error orientation (e.g. perpendicular to the vehicle heading). For KPI-2, the lateral error was defined with respect to the vehicle center of gravity, at zero look-ahead distance and perpendicular to the vehicle heading. Considering the safety aspect of KPI-3, the lateral error was defined as the perpendicular distance from the lane border to the vehicle corner closest to the lane boarder.

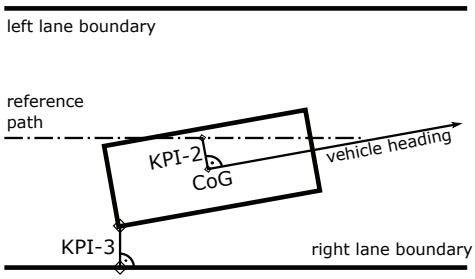

Fig. 5: Lateral position overshoot and safety distance from road lane border.

For KPI-4, the maximum allowed longitudinal acceleration/deceleration was defined according to ISO 15622:2018 norm. In this standard, the maximum allowed longitudinal acceleration and deceleration are defined as a function the ego-vehicle velocity. The values given in Table I are valid for $130\,\mathrm{km/h}$, which corresponds to the maximum velocity allowed in the examined scenario. KPI-5 was defined following ISO 21202:2020, which deals with partially automated lane change systems (PALS). For light duty vehicles, a maximal allowed lateral acceleration of $4\,\mathrm{m/s^2}$ is defined in this standard.

V. SIMULATIONS AND RESULTS ANALYSIS

In section II a test scenario according to Fig. 3 on a section of the Austrian A2 motorway was defined, which combines the two routing recommendations seen in Fig.1. Here the corresponding simulation results are given for the three different transition curves along with their comparison and evaluation according to the KPIs defined in section IV.

In the simulation the ego vehicle drives along the chosen stretch of the A2 motorway. The driving function normally keeps the vehicle in the centerline of the rightmost lane, except when an ITS-message tells the ego vehicle to use another driving strategy. According to the setup of the scenario, first a lane offset recommendation, then consequently a lane change recommendation was simulated. In Fig. 6 the simulation results for the offset from the centerline of the rightmost lane is shown. Initially the offset is zero, between $30\,\mathrm{s}$ and $90\,\mathrm{s}$ the ego vehicle receives a recommendation to drive with an in-lane offset of $40\,\mathrm{cm}$ and between $130\,\mathrm{s}$ and $160\,\mathrm{s}$ the vehicle is instructed to use the second lane. Table II gives an overview of the results of the KPI evaluation for the three different transition curve options. The main observations from this analysis and comparison will be summarised.

The maximum longitudinal velocity tracking error from set-point (KPI-1) is very small due the fact that we use constant velocity set-point and the only disturbances in the longitudinal

TABLE II: Evaluation of the KPIs for the three different transition curves.

KPI	Unit	Bezier curve	Polynomial 5^{th} order	Polynomial 4^{th} order
KPI-1	$\mathrm{km/h}$	0.09	0.10	0.10
KPI-2	cm	11	14	12
KPI-3	cm	37.8	37.8	37.8
KPI-4	$\mathrm{m/s^2}$	0.13	0.13	0.13
KPI-5	$\mathrm{m/s^2}$	2.30	2.52	2.60

dynamics are caused by steering manoeuvres. Yet there is a small difference in favor of the Bezier construct.

The maximum lateral position overshoot from set-point (KPI-2) arise during the lane change manoeuvre, as would be expected. The comparison of KPI-2 yields $11\,\mathrm{cm}$ overshoot for the Bezier curve construct, whereas $14\,\mathrm{cm}$ for the 5^{th} order polynomial, and $12\,\mathrm{cm}$ for the 4^{th} order polynomial construct. The results of all three solutions are well below the threshold of $20\,\mathrm{cm}$, yet Bezier construct had the smallest overshoot among all three. We note here that the overshoot in the maneuvers indicates that there are modelling errors in the lateral tracking controller. A linear lane-keeping model is utilized for the LQR-control design, which is clearly an over-simplification of the actual dynamics of the vehicle. However, the controller is tuned such that the overshoot is within tolerable limits.

The minimum safety distance form road lane border (KPI-3) can not be evaluated during a lane change, since the vehicle crosses the lane border during the maneuver. Therefore KPI-3 was evaluated only for the in-lane offset recommendation situation. This corresponds to the first part of the test scenario between $30\,\mathrm{s}$ to $90\,\mathrm{s}$ (see Fig. 6a). Since there is no lane change in this period, the result for the KPI-3 is the same for all the three transition curve options, therefore was not a distinguishing factor. In-lane offset must be determined as function of lane width, vehicle width and the minimum allowed safety distance from the road lane border. Minimum safety distance must also take the transient tracking errors from the lateral controller into account. To show the effect of the in-lane offset recommendation on the KPI-3, a series of simulations with varying in-lane offsets were performed. The results are given in Table III, where it can be observed that in-lane offset of up to $57\,\mathrm{cm}$ leads to fulfillment of KPI-3, given the lane width of $3.5\,\mathrm{m}$.

TABLE III: KPI-3 for different in-lane offsets.

Inlane offset	cm	20	40	60
KPI-3	cm	57.9	37.8	17.9

The maximum allowed longitudinal acceleration (KPI-4) is by far not reached. The simulation with constant velocity without traffic means the only significant disturbance is due to steering maneuvers, which led in all three simulations to the KPI-4 value of $0.13\,\mathrm{m/s^2}$.

The maximum allowed lateral acceleration (KPI-5) is also not reached by any of the three planners. The lateral acceleration is shown in Fig. 7. It can be seen that maximum

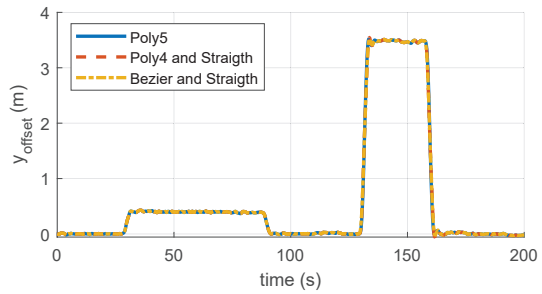

(**a**)

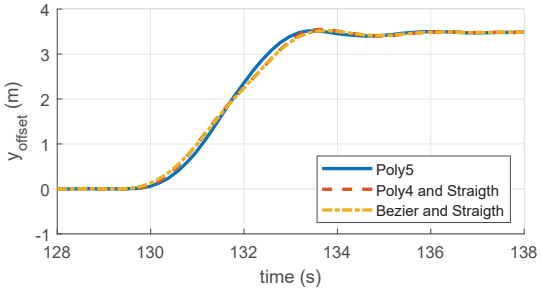

(**b**)

Fig. 6: The lateral offset from the centerline of the rightmost lane for (**a**) the whole simulation (**b**) the section of the first lane change maneuver.

acceleration is reached during lane change maneuvers. The ego vehicle travels at the rightmost lane. At about $130\,\mathrm{s}$ a lane change to the left lane is initiated and at about $157\,\mathrm{s}$ a lane change back to the rightmost lane is performed. The results of the evaluation of KPI-5 are $2.3\,\mathrm{m/s^2}$ for the Bezier curve, $2.52\,\mathrm{m/s^2}$ for the polynomial of 5^{th} order and $2.6\,\mathrm{m/s^2}$ for the construct with polynomials of 4^{th} order. The smallest lateral acceleration occurred in the planner using the Bezier curves.

VI. Conclusions

In this paper a new model for operation of automated driving functions, by utilizing specific infrastructure routing recommendations for adapting and enhancing their behavior in a context-aware fashion, was presented. The infrastructure routing recommendations are in the form of specific lane-change and in-lane offset suggestions that will be transmitted to vehicles through typical C-ITS messages such as the IVIM.

As the penetration rates of the automated vehicles (especially automated heavy-duty trucks) increase, an expedited rutting of the road surface will follow due to perfectly following the lane center-line. It is expected that the collective behavior of connected automated vehicles with the capability to adapt their behavior according to such routing recommendations will benefit both the road operators and the vehicle owners. The road operators will benefit from a gradual degradation of the road surface, while the vehicles will benefit from a safer and more comfortable ride due to avoidance of the rutted or damaged road sections as well as the blocked lanes thanks

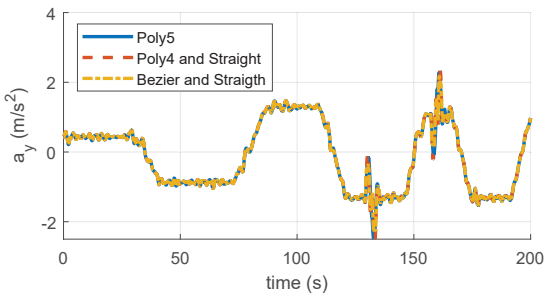

(**a**)

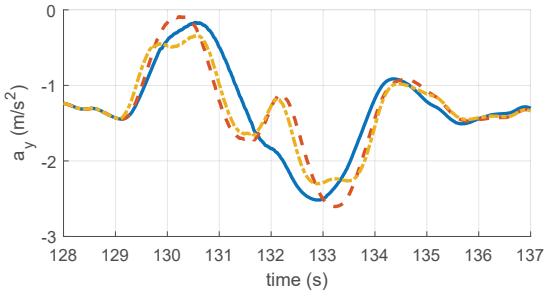

(**b**)

Fig. 7: Lateral acceleration of the ego vehicle for (**a**) the whole simulation run (**b**) the section of the first lane change maneuver.

to the routing recommendations. This is an idea being developed within the recently started EU-H2020 funded project ESRIUM, where the complete value chain for implementing this basic idea is being developed to investigate its feasibility.

In the current analysis, a specific infrastructure assisted rule-based trajectory planning scheme was presented, which utilizes three optional transition trajectories based on polynomial and Bezier curves. We also introduced the specific use cases that will be implemented in this context. The trajectory planners were developed in a high-fidelity simulation framework based on Matlab/Simulink and CarMaker software with the view of deploying the same functions in a test vehicle for real-life implementation and demonstration of the solution. This work represents a follow-up work to [5] and extends it by giving a comparison of the three alternative trajectory planners utilizing a set of performance indicators as a basis for their selection in the simulation framework. Consequently, the evaluation results were presented. Based on the analysis, the rule-based trajectory planner utilizing the quadratic Bezier-curve construct (which was also utilized in [5]) performed the best, according to the KPIs defined. Therefore, the Bezier-curve based trajectory planner will be used in the eventual real-life implementation of the algorithm.

In the future extensions, search-based optimal trajectory planners will be developed and compared with the current rule-based approach. Also, the developed trajectory planner will be imported to a real automated drive demonstrator vehicle to realize a live demonstration of the routing recommendations for representative use cases on a public road. It is planned to conduct this demonstration within the final year (2023) of the ESRIUM project.

ACKNOWLEDGMENT

This work was conducted in the scope of the ESRIUM Project, which has received funding from the European Union Agency for the Space Programme under the European Union's Horizon 2020 research and innovation programme and under grant agreement No 101004181. The content of this paper reflects only the authors' view. Neither the European Commission nor the EUSPA is responsible for any use that may be made of the information it contains. Virtual Vehicle Research GmbH has received funding within COMET Competence Centers for Excellent Technologies from the Austrian Federal Ministry for Climate Action, the Austrian Federal Ministry for Digital and Economic Affairs, the Province of Styria (Dept. 12) and the Styrian Business Promotion Agency (SFG). The Austrian Research Promotion Agency (FFG) has been authorised for the programme management.

REFERENCES

[1] INFRAMIX, "Road infrastructure ready for mixed vehicle traffic flows." https://www.inframix.eu/. accessed: 2021-09-10.

[2] M. Berrazouane, K. Tong, S. Solmaz, M. Kiers and J. Erhart, "Analysis and Initial Observations on Varying Penetration Rates of Automated Vehicles in Mixed Traffic Flow utilizing SUMO," 2019 IEEE International Conference on Connected Vehicles and Expo (ICCVE), 2019, pp. 1-7, doi: 10.1109/ICCVE45908.2019.8965065.

[3] SAE-J3016. *Surface Vehicle Recommended Practice–(R) Taxonomy and Definitions for Terms Related to Driving Automation Systems for On-Road Motor Vehicles*; Standard SAE J3016:APR2021; Society of Automotive Engineers: Warrendale, Pennsylvania, USA, 2021.

[4] ESRIUM -*EGNSS-Enabled Smart Road Infrastructure Usage and Maintenance for Increased Energy Efficiency and Safety on European Road Networks*. Available online: https://esrium.eu/ (accessed on 20 September 2021).

[5] M. Rudigier, G. Nestlinger, K. Tong, and S. Solmaz, "Development and Verification of Infrastructure-Assisted Automated Driving Functions," Electronics, vol. 10, no. 17, p. 2161, Sep. 2021. https://doi.org/10.3390/electronics10172161

[6] V. Tihanyi *et al.* "Motorway Measurement Campaign to Support R&D Activities in the Field of Automated Driving Technologies," Sensors, vol. 21, no. 6, p. 2169, Mar. 2021 [Online]. Available: http://dx.doi.org/10.3390/s21062169

[7] K. Tong, Z. Ajanovic and G. Stettinger, "Overview of Tools Supporting Planning for Automated Driving," 2020 IEEE 23rd International Conference on Intelligent Transportation Systems (ITSC), 2020, pp. 1-8, doi: 10.1109/ITSC45102.2020.9294512.

[8] D. González, J. Pérez, V. Milanés and F. Nashashibi, "A Review of Motion Planning Techniques for Automated Vehicles," in IEEE Transactions on Intelligent Transportation Systems, vol. 17, no. 4, pp. 1135-1145, April 2016, doi: 10.1109/TITS.2015.2498841.

[9] Werling, M., Ziegler, J., Kammel, S., and Thrun, S. (2010, May). Optimal trajectory generation for dynamic street scenarios in a frenet frame. In 2010 IEEE International Conference on Robotics and Automation (pp. 987-993). IEEE.

[10] Hatem Darweesh, Eijiro Takeuchi, Kazuya Takeda, Yoshiki Ninomiya, Adi Sujiwo, Luis Yoichi Morales, Naoki Akai, Tetsuo Tomizawa, and Shinpei Kato, "Open Source Integrated Planner for Autonomous Navigation in Highly Dynamic Environments," J. Robot. Mechatron., Vol.29, No.4, pp. 668-684, 2017.

[11] Rumetshofer, Johannes, Michael Stolz, and Daniel Watzenig. 2021. "A Generic Interface Enabling Combinations of State-of-the-Art Path Planning and Tracking Algorithms" Electronics 10, no. 7: 788. https://doi.org/10.3390/electronics10070788